ORIGINAL ARTICLE

Society For Biomaterials   WILEY

Evaluation of the inflammatory responses to sol–gel coatings with distinct biocompatibility levels

Andreia Cerqueira[1] | Nuno Araújo-Gomes[2] | Yang Zhang[3,4] |
Jeroen J. J. P. van den Beucken[3] | Cristina Martínez-Ramos[5] | Seda Ozturan[6] |
Raúl Izquierdo[1] | María Muriach[7] | Ricard Romero-Cano[7] | Pablo Baliño[7] |
Francisco J. Romero-Gavilán[1]

[1]Department of Industrial Systems Engineering and Design, Universitat Jaume I, Castellón de la Plana, Spain

[2]Department of Developmental Bioengineering, University of Twente, Faculty of Science and Technology, Enschede, The Netherlands

[3]Dentistry – Regenerative Biomaterials, Nijmegen, The Netherlands

[4]School of Medicine, Shenzhen University, Shenzhen, China

[5]Center for Biomaterials and Tissue Engineering, Universitat Politècnica de Valencia, Valencia, Spain

[6]Department of Periodontology, Faculty of Dentistry, Istanbul Medeniyet University, Istanbul, Turkey

[7]Unidad Pre-Departamental de Medicina, Universitat Jaume I, Castellón de la Plana, Spain

Correspondence
Francisco J. Romero-Gavilán, Department of Industrial Systems Engineering and Design, Universitat Jaume I, Campus del Ríu Sec, Avda. Vicent Sos Baynat s/n, 12071 - Castelló de la Plana, Spain.
Email: gavilan@uji.es

Funding information
Generalitat Valenciana, Grant/Award Number: GRISOLIAP/2018/091; Ministerio de Economía y Competitividad, Grant/Award Numbers: MAT2017-86043-R, RTC-2017-6147-1; Universitat Jaume I, Grant/Award Number: POSDOC/2019/28

Abstract

The immune system plays a crucial role in determining the implantation outcome, and macrophages are in the frontline of the inflammatory processes. Further, cellular oxidative stress resulting from the material recognition can influence how cell responses develop. Considering this, the aim of this study was to study oxidative stress and macrophages phenotypes in response to sol–gel materials with distinct in vivo outcomes. Four materials were selected (70M30T and 35M35G30T, with high biocompatibility, and 50M50G and 50V50G, with low biocompatibility). Gene expression, immunocytochemistry and cytokine secretion profiles for M1 and M2 markers were determined. Moreover, oxidative stress markers were studied. Immunocytochemistry and ELISA showed that 50M50G and 50V50G lead to a higher differentiation to M1 phenotype, while 70M30T and 35M35G30T promoted M2 differentiation. In oxidative stress, no differences were found. These results show that the balance between M1 and M2, more than individual quantification of each phenotype, determines a biomaterial outcome.

KEYWORDS
biomaterials, implants, inflammation, macrophage plasticity, oxidative markers

1 | INTRODUCTION

Biocompatibility describes the appropriate biological requirements of biomaterials for medical application as well as the ability of said materials to perform with an host response in a specific application.[1] It is

Andreia Cerqueira and Nuno Araújo-Gomes shares co-authorship.

determined by the coordination of the host homeostatic mechanisms, which are disturbed upon implantation, and the consequent immune response to injury.[2] The coordinated activation, type and action of highly specialized immune cells depends of the nature and site of the wound/damage.[3] Macrophages represent the first line of defense on the innate immunity, being most known by their phagocytic capabilities. Besides their major effector function of eliminating and

inactivating pathogens, these cells boost properties such as the clearance of apoptotic cells throughout the lifespan of an organism, homeostasis and activation of tissue repair processes.[4] Macrophages have the capability to enter into distinct tissues, modulate and differentiate into specialized phenotypes according to microenvironmental cues, stimuli from growth factors, cytokines, and chemokines present in biological fluids (e.g., blood). In the case of implanted biomaterials, these events are part of a whole process that could culminate in a foreign body reaction (FBR) to the material.[5] Once activated, macrophages can exhibit a spectrum of polarization states depending on their functional nature, adopting a pro-inflammatory phenotype (M1) or an anti-inflammatory phenotype (M2), with distinct surface markers and/or different gene expression profiles. When a biomaterial is implanted into the organism, this cascade of events is triggered, allowing the direct and initial migration of M1 macrophages toward the implantation site, provoking the necessary inflammatory response,[6] which is characterized by the secretion of pro-inflammatory cytokines and chemokines, such as tumor necrosis factor α (TNF-α) and interleukin 1-β (IL-1β).[7] The prolonged presence of this phenotype can lead to a state of chronic inflammation, ultimately leading to implant rejection.[8] The anti-inflammatory M2 macrophages establish themselves upon signals released by basophils, including cytokines like interleukin-10 (IL-10) and interleukin-4 (IL-4).[9] This anti-inflammatory state is distinguishable by its role on immunoregulation, matrix deposition and tissue remodeling processes.[7] The increase of M2 subsets in the biomaterial surrounding environment, toward a positive value of M2:M1 ratio, has been suggested as the key to a positive outcome of the implanted material.[10] However, the greater presence of M2 macrophages could increase of foreign body giant cells (FBGC) in situ, when its predominance is too prolonged.[5] Hence, this ratio as a marker for biocompatibility must be carefully approached.

Oxidative stress derives as a consequence of the surgical creation of a wound and implantation, being influenced by the material properties, the degree of initial inflammation and the immediate stress resulting from the procedure, occurring at all stages of the response to a biomaterial. The resulting reactive oxygen species (ROS), reactive nitrogen species (RNS) and lipid peroxidation subproducts (e.g., malondialdehyde [MDA]) act as chemo-attractants and signaling molecules during healing, and are often associated with phenotypic shifts of immune cells and modulation of cell response to a determined material.[11] Redox interactions are responsible for stabilizing these oxidation products and glutathione (GSH), synthesized from glycine, cysteine, and glutamic acid, is the most important redox-regulating thiol, acting as a substrate of glutathione peroxidase (GPx).[12] The antioxidant function of GSH is due to the oxidation of the sulfhydryl group (-SH), and the ratio between glutathione disulfide (GSSH) and GSH is an indicator of the cellular redox potential.[12] Differences in ROS generation and scavenging between M1 and M2 macrophages have been studied.[13] Superoxide generation, namely hydrogen peroxide, is typically increased and associated to the M1 macrophage phenotype, due to its phagocytic/microbiocidal activity, which depends on the synthesis of ROS and RNS. Moreover, as M2

phenotypes are usually described as being angiogenic, anti-oxidant and dependent on oxidative phosphorylation. A low expression of pro-oxidants NOX2 e NOX5 and high levels of SOD, GPx and CAT have been described as required for M2 macrophage polarization,[13] thus confirming the oxidative metabolic differences for these immune cell subpopulations.[14]

Upon implantation on a living organism, the blood is the first organic fluid in contact with the implant, leading to protein adsorption by the surface whose type, composition, quantity and conformation might impair the final outcome.[15] This process is dependent on the physicochemical characteristics of the surface of the material and can ultimately modulate macrophage and monocyte activation and migration to the implantation site.[16] In previous studies,[17] we showed that a greater deposition of complement proteins onto a biomaterial is intrinsically correlated with their biocompatibility in a living host. The oxidative stress in response to the implantation process and the material itself might also directly impair the immune cellular response/differentiation and ultimately affect the implant outcome.

Following this premise, this experimental work focuses on the study of the polarization/plasticity of activated macrophages to previously described sol–gel materials with distinct biocompatibility reactions in vivo and the correlation of between the predominance of a determined macrophage phenotype with the oxidative stress responses.

2 | MATERIALS AND METHODS

2.1 | Material selection, synthesis, and preparation

Sol–gel technology was employed to synthetize four different materials using methyltrimethoxysilane (MTMS), 3-glycidoxypropyltrimethoxysilane (GPTMS), tetraethyl orthosilicate (TEOS) and triethoxyvinylsilane (VTES) precursors in the proportions shown in Table 1. These materials, designed in previous works, were selected due to their distinct biocompatibility outcomes in vivo.[17-19] For their synthesis, the corresponding alkoxysilane amounts were diluted with 2-propanol (50% vol) and hydrolyzed adding the stoichiometric amount of acidified aqueous solution (0.1 M HNO$_3$). All the employed reagents were purchased from Sigma-Aldrich (Merck KGaA, Darmstadt, Germany). The sol–gel preparations were left stirring for 1 hr and resting for another 1 hr. The coatings were prepared immediately after this resting. For that, Grade 4 Ti discs (12 mm diameter, 1 mm thick; Ilerimplant-GMI S.L., Lleida, Spain) were employed as substrate for the coatings. Bare discs were superficially pre-treated with a sandblasting and acid-etching treatment (SAE) previously described.[20] Then, the sol–gel solutions were applied as coatings using a KSV DC dip-coater (Biolin Scientific, Stockholm, Sweden). Discs were submerged into the corresponding sol–gel (60 cm/min-speed) and kept immersed in it for 1 min. Then, the samples were taken out at 100 cm/min. Finally, heat treatments at 80°C to 70M30T and 35M35G30T, and at 140°C to 50M50G and 50V50G materials were carried out for 2 hr.

TABLE 1 Nomenclature, composition (in molar percentages) and biocompatibility of the synthetized sol–gel materials

	MTMS (%)	GPTMS (%)	VTES (%)	TEOS (%)	Biocompatibility
70M30T	70	-	-	30	High
35M35G30T	35	35	-	30	High
50M50G	50	50	-	-	Low
50V50G	-	50	50	-	Low

2.2 | In vitro assays

2.2.1 | Cell culture

For the distinct experiments, mouse murine macrophage cells (RAW 264.7) were cultured on the discs in 48-well NUNC plates (Thermo Fisher Scientific, NY) at 37°C in a humidified (95%) CO_2 incubator using as culture medium Dulbecco's Modified Eagle Medium (DMEM; Gibco, Thermo Fisher Scientific) with 10% of fetal bovine serum (FBS; Gibco) and 1% of penicillin/streptomycin (Gibco).

2.2.2 | Cell fixation for SEM imaging

After 72 hr of incubation, samples were washed once with PB 0.1 M and fixed with 3.5% glutaraldehyde for 45 min, at 37°C, in the dark. After washing twice with PB 0.1 M, the preparations were incubated with 2% osmium for 1 hr in the dark. Afterwards, samples were washed with dH_2O to eliminate any osmium residues and a chain with crescent concentrations of ethanol was performed for dehydration. The critical point drying was made through incubation with hexamethyldisilazane (HDMS; Sigma-Aldrich). Next, samples were examined in a field emission scanning electron microscope (FESEM; ULTRA 55, ZEISS Oxford Instruments) at 2 kV of voltage.

2.2.3 | Immunocytochemistry double staining

After 24 and 72 hr, samples were fixed in 4% paraformaldehyde for 10 min (Sigma-Aldrich) and washed five times in 1x PBS. The samples were blocked in 1× PBS containing 0.5% BSA and 1% Triton X-100 (Sigma-Aldrich). They were incubated with donkey anti-mouse CD206 primary antibody (Abcam, Cambridge, United Kingdom) diluted 1:250 in PBS containing 0.5% BSA and 0.5% Tween-20 (Sigma-Aldrich), overnight at 4°C. The discs were then washed five times in 1x PBS and incubated with a mixture of secondary antibodies composed of Goat anti-Donkey Biotin (Jackson ImmunoResearch Europe, Ltd., Cambridgeshire, UK) diluted 1:500 and Streptavidin Alexa Fluor 647 (Thermo Fisher Scientific) diluted 1:500 for 1 hr at room temperature. Cells were washed five times with wash buffer (1× PBS with 0.5% Triton X-100) and incubated with the primary antibody IL7-R (Santa Cruz Biotechnology, Dallas, TX) at 4°C overnight. After five washes with wash buffer, the discs were incubated with the secondary antibody Goat anti-Rabbit Alexa Fluor 488 (Thermo Fisher Scientific) for 1 hr at room temperature. After the next five washes with

wash buffer, the discs were incubated with DAPI (Roche, Basel, Switzerland) for another hour to stain the cell nuclei.

The discs were then removed from the wells, mounted on coverslipped slides with mounting medium to prevent the sample from drying out (4.8% poly[vinyl alcohol-co-vinyl acetate], 12% glycerol, 0.2 M Tris–HCl, 0.02% sodium azide) and stored at 4°C until the fluorescence microscopy analysis (Keyence International, Mechelen, Belgium).

2.2.4 | RNA extraction, cDNA synthesis and quantitative real-time PCR measurements

After 24 and 72 hr, total RNA was extracted using TRIzol (1 M guanidine thiocyanate, 1 M ammonium thiocyanate, 3 M sodium acetate, 5% glycerol, 38% aquaphenol). To each sample 300 μl of TRIzol were added followed by an incubation at room temperature. After centrifugation (5 min, 13,000 rpm, 4°C), 200 μl of chloroform were added to the supernatant, and the samples were centrifuged (5 min, 13,000 rpm, 4°C). The aqueous layer was mixed with 550 μl of isopropanol and kept at room temperature for 10 min. Samples were centrifuged (15 min, 13,000 rpm, 4°C), and washed twice with 0.5 ml of 70% ethanol. The resulting pellet was dissolved in 30 μl of RNAse free water. RNA concentration, integrity, and quality were measured using NanoVue® Plus Spectrophotometer (GE Healthcare Life Sciences, Little Chalfont, United Kingdom). Approximately 1 μg of total RNA was converted into cDNA using PrimeScript RT Reagent Kit (Perfect Real Time; TAKARA Bio Inc., Shiga, Japan) and the reaction was conducted with the following conditions: 37°C for 15 min, 85°C for 5 s and a final hold at 4°C. The resulting cDNA quality and quantity was measured using a NanoVue® Plus Spectrophotometer (GE Healthcare Life Sciences), then diluted in DNAse-free water to a concentration suitable for reliable qRT-PCR analysis and stored at −20°C.

To evaluate the effects of the materials on the inflammatory responses, genes corresponding to pro and anti-inflammatory phenotypes were selected (Table 2). *GADPH* was used as a housekeeping gene. Primers were designed using DNA sequences for these genes available from NCBI (https://www.ncbi.nlm.nih.gov/nuccore), employing PRIMER3plus software tool (http://www.bioinformatics.nl/cgi-bin/primer3plus/primer3plus.cgi) and purchased to Thermo Fischer Scientific. Quantitative real-time PCR (qRT-PCR) were carried out in 96-well plates (Applied Biosystems®, Thermo Fisher Scientific) and individual reactions contained 1 μl of cDNA, 0.2 μl of specific primers (forward and reverse at 10 μM/L) and 5 μl of SYBR Premix Ex

Phenotype	Gene symbol	Accession	Sequence
Housekeeping gene	*GADPH*	XM_017321385	F: TGCCCCCATGTTTGTGATG R: TGGTGGTGCAGGATGCATT
Pro-inflammatory (M1)	*iNOS*	NM_001313922	F: CACCTTGGAGTTCACCCAGT R: ACCACTCGTACTTGGGATGC
	TNF-α	NM_001278601	F: AGCCCCCAGTCTGTATCCTT R: CTCCCTTTGCAGAACTCAGG
	IL1-β	NM_008361	F: GCCCATCCTCTGTGACTCAT R: AGGCCACAGGTATTTTGTCG
Anti-inflammatory (M2)	*IL-10*	NM_010548	F: CCAAGCCTTATCGGAAATGA R: TTTTCACAGGGGAGAAATCG
	TGF-β	NM_011577	F: TTGCTTCAGCTCCACAGAGA R: TGGTTGTAGAGGGCAAGGAC
	EGR2	NM_001373987	F: CAGGAGTGACGAAAGGAAGC R: ATCTCACGGTGTCCTGGTTC

Taq (Tli RNase H Plus; TAKARA, Bio Inc.) in a final volume of 10 μl, and were carried out in a StepOne Plus™ Real-Time PCR System (Applied Biosystems®). The cycling parameters were an initial denaturation step (95°C, 30 s) followed by 95°C for 5 s and 60°C for 34 s, for 40 cycles. The final melt curve stage comprised a cycle at 95°C for 15 s and at 60°C, for 60 s. Fold changes were calculated using the $2^{-\Delta\Delta Ct}$ method and the data was normalized in relation to the blank wells (without any material).

2.2.5 | Cytokine quantification by ELISA

To measure secreted cytokines (TNF-α, IL-1β, TGF-β and IL-10), the cell culture supernatants used for immunocytochemistry were collected and frozen until further analysis. The concentration of these cytokines was determined using an ELISA (Invitrogen, Thermo Fisher Scientific) kit and according to the manufacturer's instructions.

2.2.6 | Oxidative stress

After 24 and 72 hr, cells were washed three times with PBS and incubated at 4°C for 10 min in lysis buffer (0.2% Triton X-100, 10 mM Tris–HCl, pH 7.2). Glutamic acid, glutathione (GSH) and glutathione disulfide (GSSG) concentrations were quantified chromatographically using the method proposed by Reed.[21] Shortly, this method is based in the reaction of the Sanger Reactant (1-fluoro-2,4-dinitrobencene) with amino groups and iodoacetic acid to block free thiol groups. Samples were measured after derivatization using a high-performance liquid chromatographic system equipped with a diode array detector. Glutathione peroxidase activity (GPx) was determined by the deseparation of NADPH monitored at 340 nm as proposed Lawrence et al.[22] Briefly, a solution containing 50 μl of samples, 550 μl of potassium phosphate buffer 0.1 M pH 7.0, EDTA 1 mM and NaN_3 1 mM was mixed with 100 μl GSH disulfide reductase (0.24 U/ml), 100 μl glutatione reduced 1 mM and 100 μl NADPH 0.15 mM. The resulting solution was incubated for 3 min at 37°C. Then, 100 μl of hydrogen peroxide 1.5 mM were added to start the reaction. Glutathione reductase activity was determined using the method proposed by Smith and et al.[23] The method consists in monitoring spectroscopically the 2-nitrobenzoic acid formation. This is formed as subproduct of the GR catalyzed reduction of GSSG to GSH in presence of 5,5′-dithiobis (2-nitrobenzoic acid) (DTNB). The GSSG reduction was started by adding 25 μl of sample to a solution containing 450 μl 0.2 M phosphate buffer pH 7.5 and 250 μl of DTNB 3 mM prepared in 10 mM phosphate buffer, 50 μl of 2 mM NADPH and 50 μl of 10 mM EDTA. Total volume was adjusted to 1 ml using ultrapure water and the wavelength set at 412 nm. MDA concentration was determined chromatographically using an HPLC system using Richard et al proposed method[24] with modifications introduced by Romero et al.[25] Sample preparation consisted in mixing samples (100 μl) with 0.75 ml of thiobarbituric acid with 0.37% and perchloric acid 6.4% (2:1, vol/vol) and heated to 95°C for an hour. Then, pH was adjusted to 6 and precipitates removed by centrifugation (10,000 rpm, 1 min). Separation was carried out in a HPLC system equipped with a C18 250 × 4.6 mm 5 μm chromatographic column using an isocratic separation. Flow was set at 1 ml/min and fluorescence detector was set to 527 nm for excitation and 532 nm for emission. Mobile phase consisted in 50 mM phosphate buffer (pH 6.0): methanol (58:42, vol/vol) and 1,1,3,3-tetramethoxypropane was used as standard solution. All standards and mobile phases were prepared daily. Protein levels were determined from cell culture lysates using a Pierce™ BCA Protein Assay Kit (Thermo Fisher Scientific) and used to normalize oxidative stress values.

2.3 | Statistical analysis

Based on the normal distribution and equal variance assumption test, the data were analyzed via one-way analysis of variance with Newman–Keuls post hoc test and expressed as mean ± *SD*. Statistical analysis was performed using GraphPad Prism 5.04 software

(GraphPad Software Inc., La Jolla, CA). The asterisk (*) indicates statistically significant ($p \leq .05$) differences between the four materials.

3 | RESULTS

3.1 | Morphological analysis

To evaluate cellular morphology, macrophages seeded on the distinct materials were studied with SEM. The obtained images of cell spreading revealed that macrophages seeded for 72 hr on 70M30T and 35M35G30T treatment acquired an elongated morphology

(Figure 1a′,b′). When seeded on 50M50G and 50V50G, macrophages adhered and spread to a typical rounded shape (Figure 1c′,d′).

3.2 | Immunocytochemistry double staining

To evaluate the expression of markers associated with M1 and M2 phenotypes, immunocytochemistry was performed. IL7-R, an M1-phenotype marker, showed significant increased fluorescence of the macrophage cultures on the 50V50G and 50M50G when compared to the other two materials (Figure 2). No differences were observed on the CD206 M2-marker fluorescence intensity.
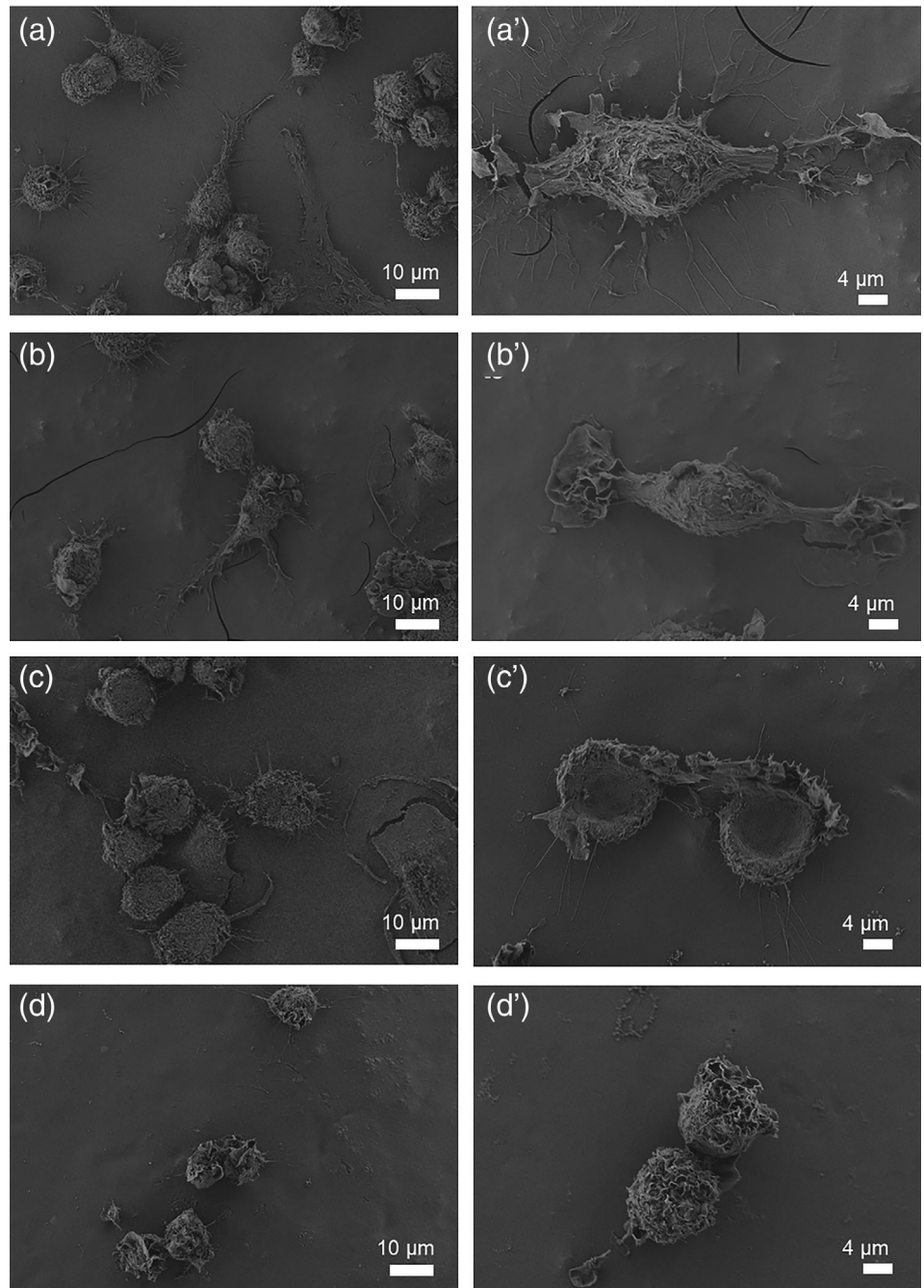

FIGURE 1 Cell morphological analysis by scanning electron microscope (SEM). Sample microphotographs of RAW 264.7 cultured on (a–a′) 70M30T, (b–b′) 35M35G30T, (c–c′) 50M50G, (d–d′) and 50V50G sol–gel hybrid coatings after 72 hr. The experiment was carried out with two replicates. Scale bar: 10 and 4 μm
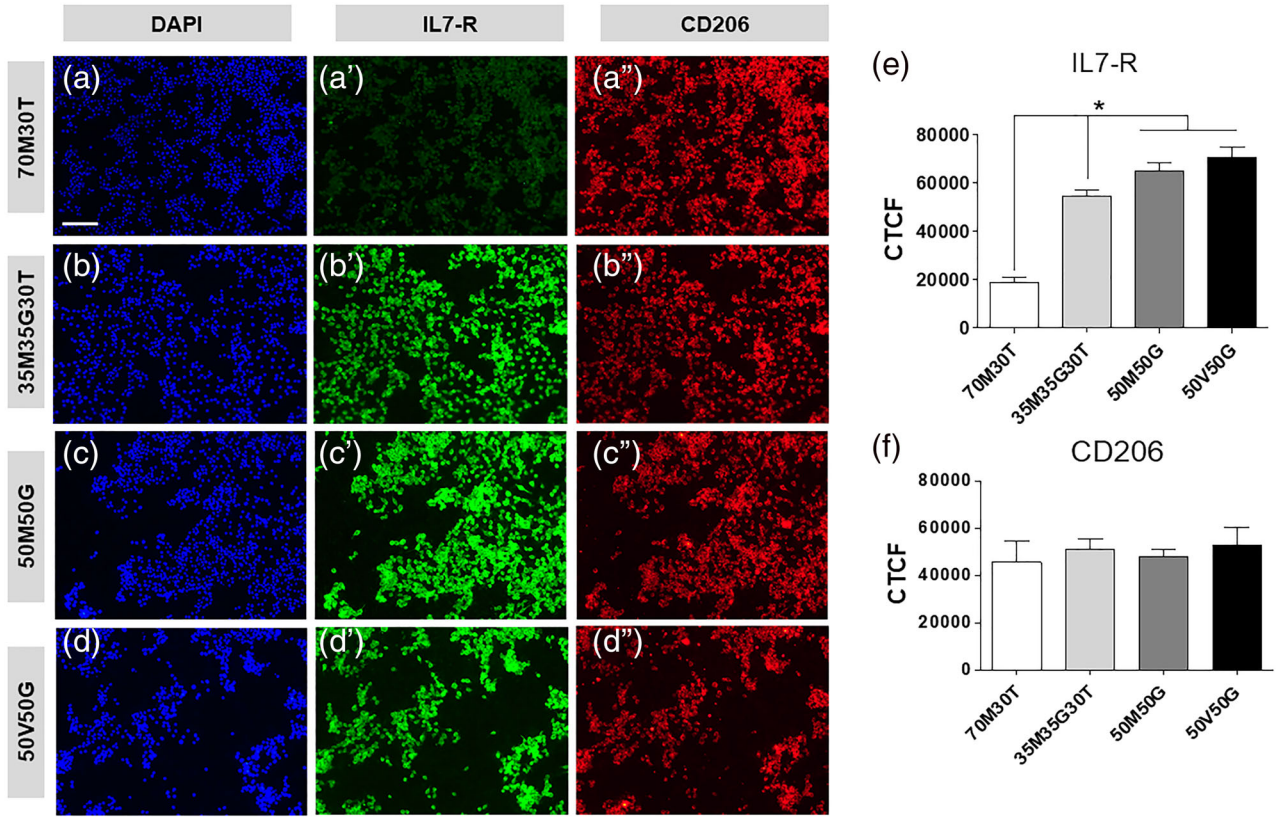
FIGURE 2 Immunostaining of RAW264.7 cells cultured on (a–a″) 70M30T, (b–b″) 35M35G30T, (c–c″) 50M50G, and (d–d″) 50V50G sol–gel hybrid coatings, after 72 hr. IL7-R (a′–d′) was used as a M1 marker and CD206 (a″–d″) was used as a M2 marker. The relative corrected total cell fluorescence (CTCF) of these markers (e and f) was quantified using ImageJ. The experiment was carried out with three replicates. Data are presented as mean ± SD. The asterisk (*) indicates differences between materials (p < .05). Scale bar: 100 μm
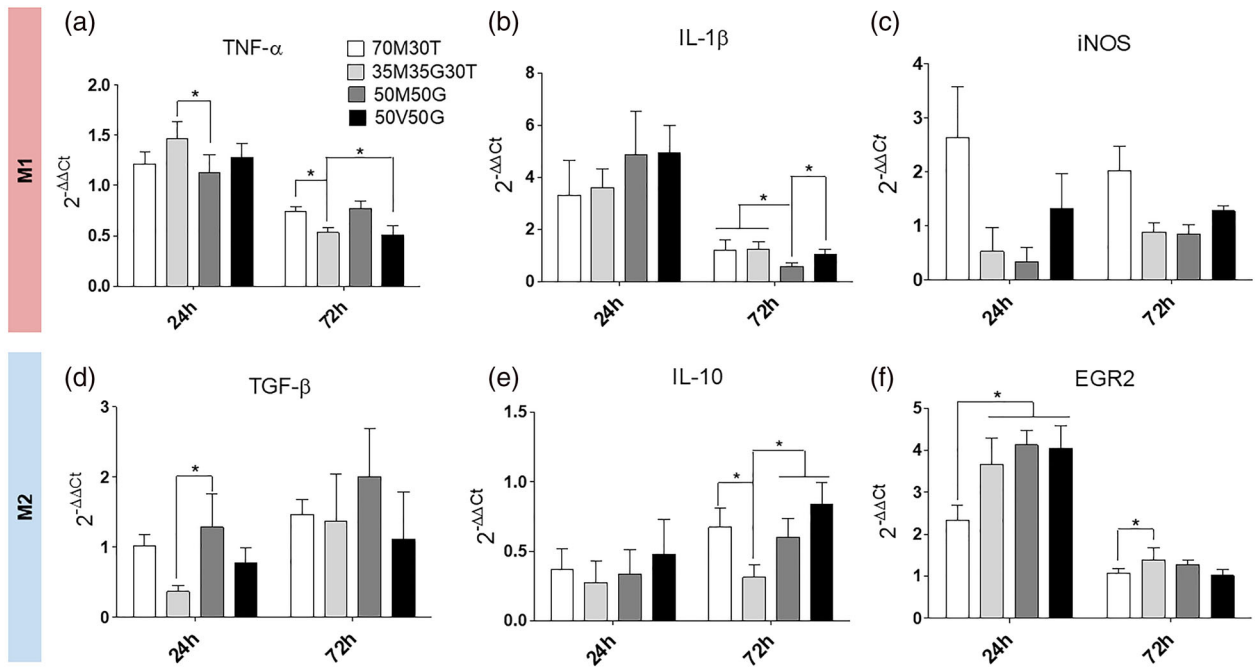

FIGURE 3 Gene expression of RAW264.7 cells cultured on 70M30T, 35M35G30T, 50M50G and 50V50G on the sol–gel hybrid coatings after 24 and 72 hr: (a) TNF-α (a), (b) IL-1β, (c) iNOS, (d) TGF-β, (e) IL10, and (f) EGR2. The experiment was carried out with six replicates. Data were normalized to blank wells (without material) and are presented as mean ± SD. The asterisk (*) indicates differences between materials (p < .05)
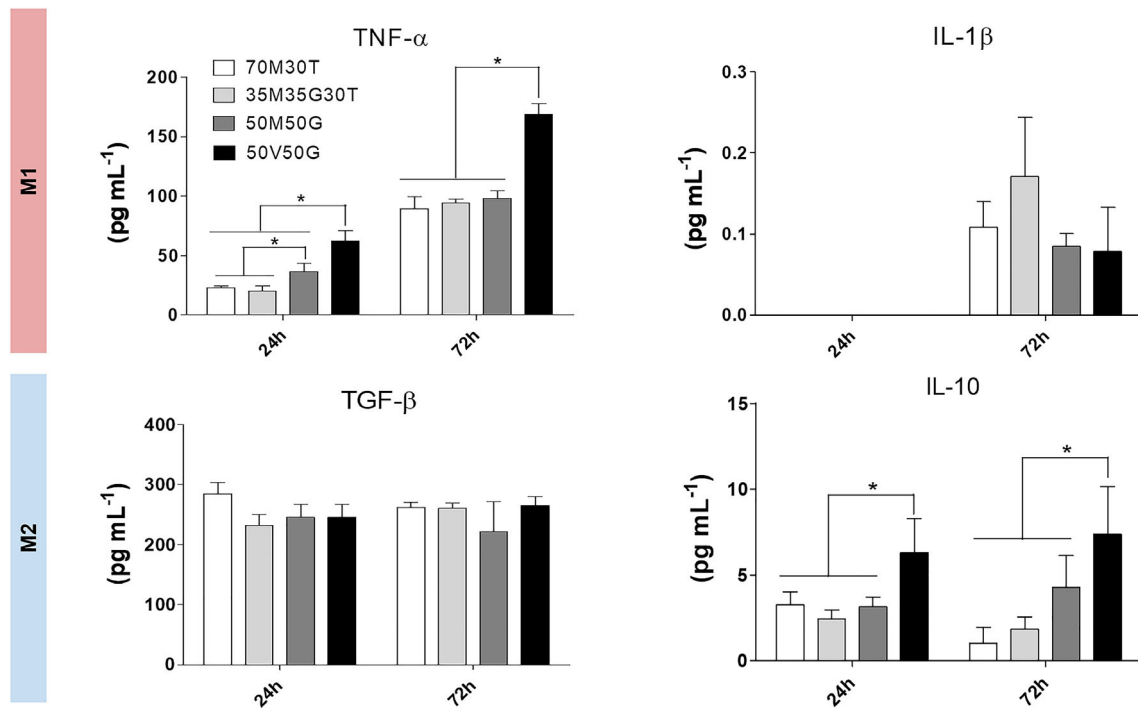
FIGURE 4 Cytokine secretion of RAW264.7 cells cultured on 70M30T, 35M35G30T, 50M50G and 50V50G on the sol–gel hybrid coatings after 24 and 72 hr: (a) TNF-α, (b) IL1-β, (c) TGF-β, and (d) IL-10. The experiment was carried out with four replicates. Data are presented as mean ± *SD*. The asterisk (*) indicates differences between materials ($p < .05$)

3.3 | Gene expression analysis

The expression of pro and anti-inflammatory markers by the RAW264.7 cells cultured onto the distinct materials is shown in Figure 3. At 24 hr, the expression of TNF-α was significantly higher on 35M35G30T, generally decreasing at 72 hr on all materials (Figure 3a). On the other hand, IL1-β expression peaked at 24 hr and then decreased on all materials at 72 hr (Figure 3b). No statistical differences were found for iNOS expression. Regarding anti-inflammatory markers, a significant increase of TGF-β was observed for 50M50G at 24 hr, but after 72 hr no differences between materials were observed (Figure 3d). The expression of IL-10 showed differences at 72 hr with a significantly higher expression on 50V50G (Figure 3e). The expression of EGR2 was significantly lower on 70M30T at 24 hr compared to the other materials and decreased at 72 hr (Figure 3f).

3.4 | Cytokine quantification by ELISA

To obtain data about inflammatory induction by these materials, secretion profiles of pro- and anti-inflammatory cytokines of RAW264.7 macrophages were assessed by ELISA (Figure 4). RAW264.7 macrophages cultured on both 50M50G and 50V50G treatments showed a clear increased secretion of TNF-α at 24 hr compared to those cultured on the 70M30T and 35M35G30T materials. At 72 hr, a marked high secretion of TNF-α for 50V50G was observed

(Figure 4a). Further, an increasing IL-10 release was observed on this material, with significance regarding the other materials (Figure 4d). IL-1β was not detected until 72 hr of culture, revealing no differences between materials.

3.5 | Oxidative stress

Figure 5 shows the macrophage oxidative stress markers (GSH, GSSG, GR, GPx and MDA) when cultured on sol–gel materials. No significant differences were found between materials at any time measured.

4 | DISCUSSION

Implanting a biomaterial foreign body into a living host leads to immediate tissue damage and cell disruption resulting from the surgical procedure. The blood protein adsorption onto the surface of the material causes platelet degranulation, forming a provisional matrix that kickstarts tissue healing responses, inducing immune cell activation and migration.[26]

The composition, conformation and amount of the bound proteins is regulated their specific affinity and the biomaterial characteristics. Distinct biological responses can result by changing the surface and consequent protein adsorption; more specifically, emerging data suggest that the modulation of immune cells is directly driven by complement protein adsorption, affecting the in vivo biocompatibility of
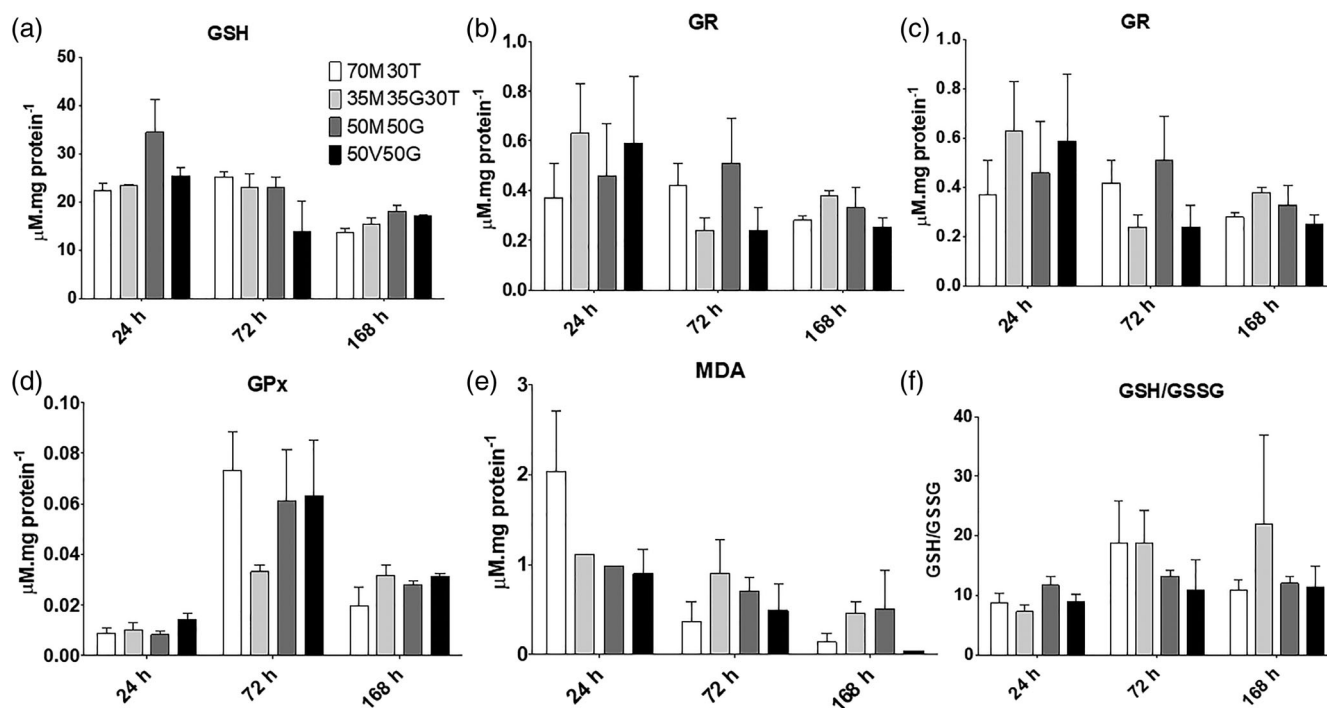
FIGURE 5   Oxidative stress markers of RAW264.7 cells cultured on 70M30T, 35M35G30T, 50M50G and 50V50G on the sol–gel hybrid coatings after 24, 72 and 168 hr: (a) GSH, (b) GSSG, (c) GR, (d) GPx, (e) MDA, (f) GSH/GSSG. The experiment was carried out with four replicates. Results are shown as mean ± *SD*

a material.[27] Immune cells interact closely with complement proteins inducing an initial inflammatory response that propagates depending on multiple factors and at implantation site activate and promote additional cellular events.

Macrophages present a high plasticity and can adopt a wide battery of phenotypes. The M1 phenotype is characterized a pro-inflammatory response, the M2 phenotype presents anti-inflammatory characteristics. At initial stages of inflammatory responses, the M1 is the most prevalent but, with time, macrophages undergo a transition to the M2 phenotype. However, the extent of the diversity of the M2 phenotype is not completely understood, and several M2 subtypes have been described (M2a, M2b, M2c, and M2d).[28] These phenotypes attenuate acute and chronic inflammation through different mechanisms and signals[29] even though this classification still fails to cover the wide range of signals and functions related to M2 macrophages.[30] With a prolonged presence of a M1 phenotype on the local microenvironment surrounding the material, fibrous structures can be observed.[5] Thus, the hypothesis that a biomaterial leading to the formation of connective tissue structures possibly induces the differentiation of macrophages to a M1 phenotype arises. Previous work has shown that the materials with low biocompatibility (50M50G and 50V50G) lead to the formation of a fibrous capsule, while the materials with good biocompatibility (70M30T and 30M35G30T) did not present inflammatory structures. To understand these distinct in vivo responses, protein adsorption of these two groups was compared. Results revealed higher adsorption of inflammatory-related proteins onto the surfaces related to biocompatibility problems.[17] The morphology acquired by macrophages when in

contact with good biocompatible materials cells displayed an elongated form, with cytoplasmic projections on the apical edges, typical of M2-phenotype; on the other hand, on the materials with low biocompatibility, the cells adopted an round shape, with very frail extensions of the cytoplasm, characteristic of a M1 phenotype.[31,32] Furthermore, higher quantities of TNF-α and IL-10 were secreted by the cells on the materials with low biocompatibility. This increased release of TNF-α, a M1 marker,[33] is observed for cells cultured on both 50M50G and 50V50G after short times of incubation (24 hr). In addition, 50V50G showed this greater cytokine liberation even after 72 hr, revealing a strong inflammatory potential with respect the other treatments. The upregulated secretion of IL-10 on 50V50G, often considered a key M2 marker,[33] is dependent on the cell line.[34] In RAW264.7 cells exposed to LPS, IL-10 secretion is increased.[35] As described in Araújo-Gomes et al,[27] GPTMS presents an epoxy ring in its structure that might mimic LPS. However, IL-10 secretion was not significantly higher on 50V50G. This might be due to the vinyl group of this formulation, as it was described to induce inflammation in hepatic murine cells.[36] These results point out that IL-10 biomarker could lead to incorrect conclusions in murine cells as it is dependent on the material chemistry. Interestingly, an overexpression of EGR2 was observed at 24 hr on the materials with low biocompatibility. The EGR2 is described to have a specific role on RAW 264.7 macrophage plasticity. Specifically, EGR2 is described to be expressed by non-activated and M2 macrophages, whereas it is downregulated in M1 macrophages,[37] being modulated by the transcription factor CEBPβ. Moreover, this gene is described as being a "master controller" of inflammation by regulating B and T cell function to achieve immune

homeostasis.[38] We hypothesize that the greater expression of this gene during the first 24 hr on the GPTMS-based materials is due to the greater inflammatory induction, to regulate and attenuate the inflammation caused by those specific materials. The immunocytochemistry supports the data obtained on by ELISA, disclosing higher tendency for the materials with low biocompatibility to induce the RAW 264.7 to differentiate toward a pro-inflammatory M1 phenotype. This distinct polarization points out to the increased inflammatory potential of the 50M50G and 50V50G coatings, which is coherent with the data obtained in a previous study and could explain the dissimilar biocompatibility associated with each of these materials.[17] However, it appears that 35M35G30T is also inducing an M1 phenotype compared to the 70M30T coating. This fact can be associated with the 35% of GPTMS incorporated in the coating network. GPTMS-derived sol–gel materials showed an increased inflammatory potential, which in turn was directly correlated with a higher affinity of complement proteins to the material surface.[27] However, when comparing to 50M50G and 50V50G, we can conclude that this may be due to the lower percentage of the compound, therefore not compromising biocompatibility.

Although this data seems to identify clear and distinct cellular behavior when exposed to the materials, these differences were not being translated into the oxidative stress induction. Data obtained from oxidative stress measurements showed no differences between materials, suggesting once more that the inflammation is driven by the complement protein attachment, consequent cytokine liberation and immune cell activation, and the materials do not represent immediate harm for the cell and/or induce oxidative stress.

5 | CONCLUSION

The aim of this study was to evaluate how sol–gel coatings with distinct in vivo outcomes modulate oxidative stress and inflammatory responses. Although there was no differences in oxidative stress, coatings with low biocompatibility (50M50G and 50V50G) had pro-inflammatory profiles with higher secretion of TNF-α. Moreover, these materials showed a higher expression of M1 receptors (IL7-R); however, the expression of M2 receptors (CD206) was not significantly different, indicating that M1 and M2 balance is key to define inflammatory responses to a biomaterial.

DATA AVAILABILITY STATEMENT
The data that support the findings of this study are available from the corresponding author upon reasonable request.

ORCID
Jeroen J. J. P. van den Beucken   https://orcid.org/0000-0002-0301-1966
Francisco J. Romero-Gavilán   https://orcid.org/0000-0001-8300-7248

REFERENCES

1. Anderson JM. *Biocompatibility*. Polymer Science: A Comprehensive Reference (Vol. 9, pp. 363-383). Amsterdam, The Netherlands: Elsevier; 2012.
2. Anderson JM, McNally AK. Biocompatibility of implants: lymphocyte/macrophage interactions. *Semin Immunopathol*. 2011;33: 221-233.
3. Chen L, Deng H, Cui H, et al. Inflammatory responses and inflammation-associated diseases in organs. *Oncotarget*. 2018;9(6): 7204-7218.
4. Martinez FO. Macrophage activation and polarization. *Front Biosci*. 2008;13:453.
5. Anderson JM, Rodriguez A, Chang DT. Foreign body reaction to biomaterials. *Semin Immunol*. 2008;20:86-100.
6. Classen A, Lloberas J, Celada A. Macrophage activation: classical vs alternative. *Methods Mol Biol*. 2009;531:29-43.
7. Mantovani A, Sica A, Sozzani S, Allavena P, Vecchi A, Locati M. The chemokine system in diverse forms of macrophage activation and polarization. *Trends Immunol*. 2004;25:677-686.
8. Sheikh Z, Brooks PJ, Barzilay O, Fine N, Glogauer M. Macrophages, foreign body giant cells and their response to implantable biomaterials. *Materials (Basel)*. 2015;8:5671-5701.
9. Varin A, Gordon S. Alternative activation of macrophages: immune function and cellular biology. *Immunobiology*. 2009;214:630-641.
10. Brown BN, Londono R, Tottey S, et al. Macrophage phenotype as a predictor of constructive remodeling following the implantation of biologically derived surgical mesh materials. *Acta Biomater Acta Mater*. 2012;8:978-987.
11. Thomsen P, Gretzer C. Macrophage interactions with modified material surfaces. *Curr Opin Solid State Mater Sci*. 2001;5:163-176.
12. Krifka S, Spagnuolo G, Schmalz G, Schweikl H. A review of adaptive mechanisms in cell responses towards oxidative stress caused by dental resin monomers. *Biomaterials*. 2013;34(19):4555-4563.
13. Griess B, Mir S, Datta K, Teoh-Fitzgerald M. Scavenging reactive oxygen species selectively inhibits M2 macrophage polarization and their pro-tumorigenic function in part, via Stat3 suppression. *Free Radic Biol Med*. 2020;147:48-60.
14. Wang F, Zhang S, Vuckovic I, et al. Not a requirement for M2 macrophage differentiation. *Cell Metab*. 2018;28:463-475.e4.
15. Araújo-Gomes N, Romero-Gavilán F, Sanchez-Pérez AM, et al. Characterization of serum proteins attached to distinct sol–gel hybrid surfaces. *J Biomed Mater Res B Appl Biomater*. 2017;106(4): 1477-1485.
16. Sridharan R, Cameron AR, Kelly DJ, Kearney CJ, O'Brien FJ. Biomaterial based modulation of macrophage polarization: a review and suggested design principles. *Mater Today*. 2015;18:313-325.
17. Romero-Gavilán F, Sanchez-Pérez AM, Araújo-Gomes N, et al. Proteomic analysis of silica hybrid sol-gel coatings: a potential tool for predicting the biocompatibility of implants in vivo. *Biofouling*. 2017;In press;33:676-689.
18. Araújo-Gomes N, Romero-Gavilán F, García-Arnáez I, et al. Osseointegration mechanisms: a proteomic approach. *J Biol Inorg Chem*. 2018;23:459-470.
19. Romero-Gavilan F, Araújo-Gomes N, Sánchez-Pérez AM, et al. Bioactive potential of silica coatings and its effect on the adhesion of proteins to titanium implants. *Colloids Surf B Biointerfaces*. 2017;162: 316-325.

20. Romero-Gavilán F, Gomes NC, Ródenas J, et al. Proteome analysis of human serum proteins adsorbed onto different titanium surfaces used in dental implants. *Biofouling*. 2017;*33*:98-111.

21. Reed DJ, Babson JR, Beatty PW, Brodie AE, Ellis WW, Potter DW. High-performance liquid chromatography analysis of nanomole levels of glutathione, glutathione disulfide, and related thiols and disulfides. *Anal Biochem*. 1980;*106*:55-62.

22. Lawrence RA, Parkhill LK, Burk RF. Hepatic cytosolic non selenium-dependent glutathione peroxidase activity: its nature and the effect of selenium deficiency. *J Nutr*. 1978;*108*:981-987.

23. Smith IK, Vierheller TL, Thorne CA. Assay of glutathione reductase in crude tissue homogenates using 5,5′-dithiobis(2-nitrobenzoic acid). *Anal Biochem*. 1988;*175*:408-413.

24. Richard MJ, Guiraud P, Meo J, Favier A. High-performance liquid chromatographic separation of malondialdehyde-thiobarbituric acid adduct in biological materials (plasma and human cells) using a commercially available reagent. *J Chromatogr B Biomed Sci Appl*. 1992;*577*:9-18.

25. Romero FJ, Bosch-Morell F, Romero MJ, et al. Lipid peroxidation products and antioxidants in human disease. *Environ Health Perspect*. 1998;*106*:1229-1234.

26. Romero-Gavilán F, Araújo-Gomes N, Cerqueira A, et al. Proteomic analysis of calcium-enriched sol–gel biomaterials. *J Biol Inorg Chem*. 2019;*24*:563-574.

27. Araújo-Gomes N, Romero-Gavilán F, Zhang Y, et al. Complement proteins regulating macrophage polarisation on biomaterials. *Colloids Surf B Biointerfaces*. 2019;*181*:125-133.

28. Witherel CE, Sao K, Brisson BK, et al. Regulation of extracellular matrix assembly and structure by hybrid M1/M2 macrophages. *Biomaterials*. 2021;*269*:120667.

29. Klopfleisch R. Macrophage reaction against biomaterials in the mouse model—phenotypes, functions and markers. *Acta Biomater*. 2016;*43*:3-13.

30. Roszer T. Understanding the mysterious M2 macrophage through activation markers and effector mechanisms. *Mediators Inflamm*. 2015;816460.

31. McWhorter FY, Wang T, Nguyen P, Chung T, Liu WF. Modulation of macrophage phenotype by cell shape. *Proc Natl Acad Sci USA*. 2013;*110*:17253-17258.

32. Jia Y, Yang W, Zhang K, et al. Nanofiber arrangement regulates peripheral nerve regeneration through differential modulation of macrophage phenotypes. *Acta Biomater Acta Mater*. 2019;*83*:291-301.

33. Gu Q, Yang H, Shi Q. Macrophages and bone inflammation. *J Orthop Transl*. 2017;*10*:86-93.

34. Spiller KL, Nassiri S, Witherel CE, et al. Sequential delivery of immunomodulatory cytokines to facilitate the M1-to-M2 transition of macrophages and enhance vascularization of bone scaffolds. *Biomaterials*. 2015;*37*:194-207.

35. Pengal RA, Ganesan LP, Wei G, Fang H, Ostrowski MC, Tridandapani S. Lipopolysaccharide-induced production of interleukin-10 is promoted by the serine/threonine kinase Akt. *Mol Immunol*. 2006;*43*:1557-1564.

36. Anders LC, Lang AL, Anwar-Mohamed A, et al. Vinyl chloride metabolites potentiate inflammatory liver injury caused by LPS in mice. *Toxicol Sci*. 2016;*151*:312-323.

37. Veremeyko T, AWY Y, Anthony DC, Strekalova T, Ponomarev ED. Early growth response gene-2 is essential for M1 and M2 macrophage activation and plasticity by modulation of the transcription factor CEBPβ. *Front Immunol*. 2018;*9*:2515.

38. Li S, Miao T, Sebastian M, et al. The transcription factors Egr2 and Egr3 are essential for the control of inflammation and antigen-induced proliferation of B and T cells. *Immunity*. 2012;*37*:685-696.